HHS Public Access

Author manuscript

Nano Lett. Author manuscript; available in PMC 2021 March 18.

Published in final edited form as:

Nano Lett. 2019 January 09; 19(1): 173–181. doi:10.1021/acs.nanolett.8b03585.

Spontaneous Nucleation of Stable Perfluorocarbon Emulsions for Ultrasound Contrast Agents

David S. Li[1,2], **Sarah Schneewind**[1], **Matthew Bruce**[3], **Zin Khaing**[4], **Matthew O'Donnell**[2], **Lilo Pozzo**[1,*]

[1]Department of Chemical Engineering, University of Washington, Seattle, WA

[2]Department of Bioengineering, University of Washington, Seattle, WA

[3]Center for Industrial and Medical Ultrasound, Applied Physics Lab, University of Washington, Seattle, WA

[4]Department of Neurological Surgery, University of Washington, Seattle, WA

Abstract

Phase-change contrast agents are rapidly developing as an alternative to microbubbles for ultrasound imaging and therapy. These agents are synthesized and delivered as liquid droplets and vaporized locally to produce image contrast. They can be used like conventional microbubbles, but with the added benefit of reduced size and improved stability. Droplet-based agents can be synthesized with diameters on the order of 100 nm, making them an ideal candidate for extravascular imaging or therapy. However, their synthesis requires low boiling point perfluorocarbons (PFCs) to achieve activation (i.e. vaporization) thresholds within FDA approved limits. Minimizing spontaneous vaporization while producing liquid droplets using conventional methods with low boiling point PFCs can be challenging. In this study, a new method to produce PFC nanodroplets using spontaneous nucleation is demonstrated using PFCs with boiling points ranging from −37°C to 56°C. Sometimes referred to as the ouzo method, the process relies on saturating a co-solvent with the PFC before adding a poor solvent to reduce solvent quality, forcing droplets to spontaneously nucleate. This approach can produce droplets ranging from under 100 nm to over 1 μm in diameter. Ternary plots showing solvent and PFC concentrations leading to droplet nucleation are presented. Additionally, acoustic activation thresholds and size distributions with varying PFC and solvent conditions are measured and discussed. Finally, ultrasound contrast imaging is demonstrated using ouzo droplets in an animal model.

Keywords

Ultrasound; contrast agents; nanodroplets; phase-change

*Corresponding Author: Prof. Lilo Pozzo (dpozzo@uw.edu, Phone: 206-685-8536).

Supporting Information:

Full ouzo phase diagrams (figure S1) and video showing activated nanodroplets perfusing through the spinal cord vasculature (video S1).

Perfluorocarbon (PFC) gas filled microbubbles are a medically approved contrast agent for diagnostic ultrasound imaging. In addition to vascular and cardiac imaging, microbubbles are also being tested for drug delivery and cavitation-based therapies.[1–4] They are typically constrained to endovascular applications because of their large size (>1μm in diameter). Because of recent interest in microbubbles for ultrasound-based theranostics (combining diagnostic imaging with therapy), great effort has been made in synthesizing microbubbles small enough to diffuse between tight junctions and penetrate into diseased tissues. To freely diffuse past the vessel walls and into tissue, agents must be smaller than ~200 nm in diameter.[3–5] Producing such agents has proven difficult because bubbles at those scales are unstable and have short lifetimes due to accelerated dissolution into the surrounding liquid due to a higher Laplace pressure.[4,6–8] Moreover, several studies have concluded that as the bubble diameter decreases, the effective membrane stiffness increases. This in turn causes an increase in bubble resonant frequency and reduced echogenic properties. [6–8]

Liquid PFC nanodroplets have been proposed as an alternative to gaseous microbubbles for medical ultrasound applications. As liquid droplets, the emulsions can be stable for days or weeks.[9–12] Moreover, prior to activation, they are transparent to ultrasound and provide no ultrasound imaging contrast.[10,11,13] However, upon applying a high amplitude acoustic pulse, droplets can be selectively vaporized in a region of interest to form bubbles that are up to five times diametrically larger than the initial droplet.[10,14–18] After ‘activation’, the gas micro-/nano-bubbles can be used in the same manner as conventional microbubbles.[11,19–21] In addition to contrast enhanced imaging, phase-change contrast agents have also been actively researched in therapeutic ultrasound applications including embolotherapy[22–24], histotripsy[25,26], drug delivery[9,27], and photoacoustic imaging[28–30].

Several other studies have successfully demonstrated that PFC droplets with diameters under 200 nm can be produced from various different methods.[21,29–32] Such small droplets can diffuse out of blood vessels and into tissues for extravascular imaging and/or therapy.[3–5] However, as the droplet diameter decreases, they also experience a stabilizing effect preventing spontaneous vaporization and an increase in the acoustic activation threshold.[12,13,17,33] Currently, there are two debated mechanisms for explaining the increased stability of nanoemulsions: increased contributions from the Laplace pressure [10] and homogenous nucleation [12]. The long standing hypothesis has been that the increase in Laplace pressure with reducing droplet diameter results in an increase in internal pressure in the droplet and thus a suppression of boiling.[10,17] However, recent results from Mountford and Borden shows that the Laplace pressure does not sufficiently explain the enhanced droplet stability.[12] Instead, homogeneous nucleation theory predicts a much greater energy barrier to droplet vaporization that better matches experimental measurements.[12] Regardless, the Laplace pressure and homogeneous nucleation theory both suggest an increase in droplet stability with decreasing diameter, requiring an increase in acoustic pressure needed to initiate droplet vaporization, potentially to levels beyond FDA limits.[19–21,31,34,35] The FDA limit is defined as the MI<1.9, where $MI = P/\sqrt{f}$, P is the peak negative pressure in MPa and f is the frequency in MHz. [36] Although superharmonic focusing of the acoustic wave in droplets leads to a decrease in acoustic vaporization threshold with increasing frequency, which can reduce the activation threshold to within FDA limits, a reduction in focal gain is observed

when the droplet much smaller than an acoustic wavelength (e.g. nanodroplets). [15,17,37] Low boiling point PFCs can help reduce the vaporization threshold to within FDA limits.[19–21,31] Often, natively gaseous PFCs must be used to synthesize nanodroplets with a sufficiently low acoustic pressure threshold for clinical purposes.[20,21]

Unfortunately, it can be very challenging to maintain low boiling point PFCs, such as perfluorobutane ($T_{Boiling}$ = −2°C) and perfluoropropane ($T_{Boiling}$ = −37°C), in their liquid phase during droplet synthesis using conventional methods such as sonication, high-speed shaking, and homogenization.[11,20,31,34] In some cases, cryogenic conditions must be maintained during emulsification.[11] Alternatively, condensing microbubbles to form nanodroplets is sometimes used to form nanodroplets from low boiling point PFCs.[19–21,38] However, microbubble condensation is limited to gaseous PFCs.[11]

In this study, an alternative method of synthesizing PFC nanodroplets through spontaneous droplet nucleation is demonstrated. In colloid science, this has been coined the ‘ouzo effect’ after the opacity change due to the spontaneous formation of anise oil droplets when water is added to the Greek alcoholic drink, ouzo.[5,31,39,40] In general, this method has two steps beginning with dissolving the oil (PFC) into a ‘good’ solvent (alcohol), which is also completely miscible with a ‘poor’ co-solvent (water). To nucleate the droplets, the ‘poor’ solvent is simply added to the dissolved oil in the ‘good’ solvent. By adding water to the PFC/alcohol solution, the oil solubility is rapidly reduced, forcing the oil phase out of solution and spontaneously nucleating droplets with surprising monodispersity and stability. In this study, ternary phase diagrams showing the solvent conditions necessary to nucleate PFC droplets are presented. In addition, droplet size distribution, stability, and activation thresholds for contrast agents are discussed. Finally, ultrasound imaging using ouzo PFC droplets is demonstrated in an animal model.

PFC ouzo droplets were synthesized by first dissolving a PFC into ethanol (co-solvent). A maximum of approximately 2.0% perfluorohexane (C_6F_{14}, $T_{Boiling}$ = 56°C), 2.3% perfluoropentane (C_5F_{12}, $T_{Boiling}$ = 29°C), 2.5% perfluorobutane (C_4F_{10}, $T_{Boiling}$ = −2°C), and 2.7% perfluoropropane (C_8F_8, $T_{Boiling}$ = −37°C) by volume could be dissolved in ethanol. In the ethanol phase, a 20:1 mole ratio of dipalmitoylphosphatidylcholine (DPPC) and N-(Methylpolyoxyethylene oxycarbonyl)-1,2-distearoyl-sn-glycero-3-phosphoethanolamine sodium salt (DSPE-PEG 2K) lipids were also dissolved. The total lipid concentration was varied from 0.10 mg/ml to 1.82 mg/ml depending on the volume of perfluorocarbon that was used. Lipid concentration much less 0.10 mg/ml still resulted in stable emulsions. However, lower concentration lipids solutions were not used to ensure ample lipids were in solution to stabilize the droplet interface. Droplet formulations using greater lipid concentration in solution resulted in the formation of lipid aggregates and destabilizing droplets through flocculation. When an aqueous solution (solvent) prepared at a ratio of 7:2:1 water/propylene glycol/glycerol is added to the PFC/ethanol solution, the PFC oil phase quickly loses solubility resulting in the spontaneous nucleation of stable droplets (Figure 1). Since PFCs are known to have very poor solubility in water, the greater the water content relative to ethanol, the lower the PFC solubility is in the final mixed solvent. It is important to note that the inclusion of glycerol and propylene glycol was not essential for droplet nucleation. In fact, PFC emulsions can also be generated in the absence

of any stabilizer (Figure S2 and S3 Supplemental Information). However, glycerol and propylene glycol are commonly used along with lipid mixtures to greatly improve microbubble stability.[41,42] Here, glycerol and propylene glycol were also included in the ouzo droplet formulation to make the agent composition analogous to microbubbles and to increase stability.

A ternary phase diagram indicating the volume percentages of PFC oil, ethanol, and water solution ($\%_{Water} = 100\% - \%_{Ethanol} - \%_{PFC}$) that is required to nucleate droplets was created for each of the PFCs tested (Figure 2. Full ouzo ternary plots appear in supplemental Figure S1). For all PFCs, a minimum water concentration was required to nucleate droplets. As the PFC concentration was reduced, a proportionally greater concentration of water was required to nucleate PFC droplets. Comparing the conditions using different PFCs, the size of the ouzo region for increasingly volatile PFCs (i.e. PFH to OFB) decreased. The reduced ouzo region in the ternary plot is likely due to an increase in PFC oil solubility in both ethanol and water with decreasing PFC molecular weight (i.e. increased volatility). This is also supported by the thermodynamics of cavity formation. Because larger molecular weight PFCs displace a larger number of water molecules than an equal number of a lower molecular weight PFC, the solvent conditions are less favorable for large molecular weight PFCs to stay in solution than low molecular weight ones.[43] This results in the larger molecular weight PFCs having a larger ouzo region than the lower molecular weight PFCs.

Although the PFC type also plays a small role in determining droplet size, the size distributions were primarily correlated to the PFC concentration and the ethanol/water ratio used to induce spontaneous emulsification (figure 3). Nanodroplets with diameters on the order of 100 nm could be easily synthesized using all perfluorocarbons tested (figure 3A). Moreover, ouzo-synthesized droplets of ~100 nm in diameter were found to be stable for days or weeks depending on the storage conditions (figure 3B).

Zeta potential measurements also suggest that lipids successfully coated the droplet interface as they do with microbubbles (supporting figure S2). The zeta potential increased from −23 mV for uncoated droplets to −9.93 mV for DPPC and DPSE-PEG coated droplets and 3.9 mV for DPPC coated droplets. Prior to measuring the zeta potential of the lipid coated droplets, the samples were centrifuged, to remove excess lipids in solution, and redispersed. This process was repeated three times to ensure all excess lipids were removed and the zeta potential measurements were of the droplets. The zeta potentials of both lipid coated droplets were statistically different from that of uncoated ones. Moreover, lipid coated droplets matched the zeta potentials of lipid micelle samples, suggesting that the droplets were coated with lipids. In the absence of the lipid shell, DLS measurements revealed a rapid increase in size in the droplet distribution, which was not seen with lipid coated droplets (supporting figure S3). The increase in uncoated droplet size was likely due to a combination of coalescence in the short time scale and Ostwald ripening over the longer time scales. In contrast, lipid coated droplets had nearly no change in size throughout the same time scale, suggesting that lipids prevent unwanted coalescence.

Perfluorohexane was also used as a representative PFC to further investigate changes in droplet size distribution as a function of oil concentration and relative ethanol-to-water ratios

(figure 3C). In general, as PFC saturation in ethanol increased, the average droplet size also increased. This result was expected because a solution with a higher PFC concentration would have more PFC pushed out of solution than a lower concentration solution for any given volume of water added.

Water concentrations between 30-60 volume % generally resulted in the largest nucleated droplets, while the smallest droplets were observed at the extremes of the lowest and highest water and ethanol concentrations. The increase in droplet diameter with increasing water concentration (i.e. lower ethanol concentration) is expected. As more water was introduced into the sample, the solvent phase became a poorer solvent for dissolved PFC. As a result, a greater concentration of PFC lost solubility with increasing water concentration, producing larger droplets. However, if the water concentration was sufficiently high (i.e. ethanol concentration <35%), the droplet diameter again started to decrease with increasing water concentration. At the lowest ethanol concentrations, droplet nucleation was likely limited by diffusion due to the low PFC concentrations present. This limited the concentration of PFC molecules within a finite diffusion radius of growing drop nuclei, producing smaller droplets at lower ethanol (i.e. lower PFC/higher water) concentrations.

A similar effect was observed by Vitale and Katz[39], who investigated ouzo droplet nucleation of divinyl benzene droplets in water. In their study, they noted that the resulting droplet diameter was directly related to concentration of excess oil pushed out of solution when the poor solvent was introduced. [39] Although we were unable to estimate the volume of excess PFC oil pushed out of solution to nucleate droplets, a similar effect likely occurred with PFC ouzo droplets. At one extreme, when the ethanol concentration was low, overall oil concentration was also low. At the opposite extreme, when the ethanol concentration was high, it is plausible that only a low amount of PFC was forced out of solution while the majority of PFC was still dissolved in the continuous phase. Thus, at both extremes, a low volume of excess PFC oil is forced out of solution and small droplets are produced.

Although PFC concentrations in solution after synthesis were typically under 1 vol. %, the number concentration of droplets formed using the ouzo synthesis method was as high as 10^{12} droplet/ml. The droplet concentrations were estimated based off of back calculations from the volume of PFC dissolved, the droplet size distribution measured, and assuming that all the PFC was pushed out of solution to form droplets. Gravimetric measurements showed little PFC loss is observed with the ouzo synthesis method, because little mechanical energy or heat is generated during droplet nucleation. In contrast, during emulsification via sonication or homogenization, PFC losses up to 80% occur because input energy can vaporize large amounts of volatile oils. [44] Depending on droplet size and ethanol content used during synthesis, final droplet concentrations in this work varied from 10^{10} droplet/ml (typical for ~1 μm diameter droplets) to up to 10^{12} droplet/ml (common for ~100 nm diameter droplets).

Activation thresholds for droplets synthesized with various PFC were also measured using an acoustic cavitation setup. The droplets were activated using short pulses (15 cycles) from a 1.24 MHz focused transducer in a degassed water bath held at body temperature (37°C). The 50% activation (cavitation) threshold for perfluorohexane ($T_{Boiling}$ = 56°C),

perfluoropentane ($T_{Boiling}$ = 29°C), perfluorobutane ($T_{Boiling}$ = −2°C), and perfluoropropane ($T_{Boiling}$ = −37°C) were 6.86 MPa, 5.11 MPa, 3.49 MPa, and 1.74 MPa (figure 4A), respectively. The pressure threshold to vaporize droplets was directly correlated with the boiling point of the PFC, as the boiling point is an indicator of PFC volatility. These thresholds are in line with similar PFC droplet formulations of Sheeran *et al.*, who used microbubble condensation to produce droplets with gaseous PFCs and an extruder for liquid PFCs.[20,21]

The activation threshold of ouzo PFC droplets could also be modulated using PFC blends (figure 4B). This was demonstrated by combining a high boiling point PFC (perfluorohexane) with a low boiling point PFC (perfluoropropane). The blended droplets were prepared by saturating two ethanol solutions separately, each with a different perfluorocarbon, and combining the two ethanol-PFC solutions to the desired mixture ratio prior to adding the water mixture to nucleate droplets. As the perfluoropropane concentration increased, the activation threshold decreased. Fitting a linear function between the cavitation thresholds of perfluorobutane and pefluorohexane revealed that the activation threshold of the PFC blended droplets was well predicted based on a volume fraction weighted sum of the activation thresholds of the PFCs used (R^2 = 0.97). Having the option to tune the activation threshold using PFC blends would be beneficial in scenarios where a specific activation threshold is needed to optimize droplet stability and activation sensitivity.

Ouzo-synthesized droplets were used as an ultrasound contrast agent in a rat spinal cord model (figure 5). Surgical procedures were performed according to approved institutional animal care and use committee (IACUC) protocol following all appropriate guidelines from the university's Animal Welfare Assurance (A3464–01) as well as the NIH Office of Laboratory Animal Welfare (OLAW). A laminectomy was performed to remove the top surface of spine vertebrae, exposing the spinal cord. A bolus injection of perfluorobutane droplets ($T_{Boiling}$ = 29°C) with a mean diameter of 182 nm was administered via tail vein and imaged using a 15 MHz linear array ultrasound transducer. Spinal cord tissue was seen at a depth between approximately 4 and 7 mm from the transducer face (figure 5C) on top of the vertebral bones of the spine. Although contrast from the droplets could not be easily seen in conventional B-mode imaging (figure 5C), the agent was easily visualized using harmonic imaging (figure 5B and 5C, see supplemental media). Harmonic imaging was necessary to suppress intrinsic linear signals from this tissue model and to highlight the non-linear signals that are generated from bubble oscillations.[45,46] Detection of a harmonic signal after injection strongly suggests that droplets were successfully converted into microbubbles. Maximum intensity projections (figure 5D) over a one second interval flowing bubble activation revealed the branched microvasculature of the spinal cord. Such images are a classical example of contrast-enhanced ultrasound (CEUS) images revealing details of tissue microcirculation.

At the frequency used, a low boiling point PFC droplet with a low activation threshold was needed for *in vivo* experiments because the pressure output from the high-frequency transducer was relatively low. Injections of higher boiling point PFCs, such as perfluoropentane ($T_{Boiling}$ = 29°C) and perfluorohexane ($T_{Boiling}$ = 56°C), provided nearly zero contrast enhancement since they were not activated by the clinical imaging transducer.

Based on these results, high volatility PFCs such as perfluorobutane ($T_{Boiling}$ = −2°C) and perfluoropropane ($T_{Boiling}$ = −37°C) are better suited for contrast-enhanced imaging using existing clinical imaging ultrasound due to their low acoustic activation thresholds. Having a low acoustic activation threshold would enable deeper droplet activation contrast enhanced imaging without exceeding FDA thresholds imposed on acoustic pressure. However, to develop the pressures needed to vaporize droplets several centimeters into tissue, a lower frequency transducer in the range of 4-8 MHz would be better suited than a 15 MHz transducer. By shifting to lower frequency transducers, acoustic attenuation would be reduced, and higher driving voltages could be achieved, resulting in greater acoustic pressures at depth. Moreover, although we were unable to vaporize the higher boiling point PFCs with the 15 MHz imaging probe, it is possible that by using a lower frequency transducer the increased acoustic pressures at depth may be enough to vaporize higher boiling point perfluoropentane and perfluorohexane based droplets. From the literature, these agents quickly recondense back into their liquid phase after vaporization. [28,30,32,38,47,48] Reversible vaporization and condensation has been shown to be beneficial in extending the lifetime of the agents after repeated activation cycles. [28,31,32,49]

A new method to produce perfluorocarbon droplets using spontaneous nucleation has been developed and presented. The ouzo method is a fast and easy approach to produce nanodroplets with minimal equipment requirements and low costs. Although it was demonstrated here using fully fluorinated PFCs with boiling points ranging from −37°C up to 56°C, the method can be extended to other types of PFCs or oils. Even though lipids were used in this study as a coating material, any alcohol or water-soluble surfactant material can be used. Methods for polymerizing shells [31] on the droplet interface and/or the addition of targeting peptides can be easily adapted and incorporated into the ouzo method to produce PFC droplet based contrast agents for applications requiring agents with diameters less than 200 nm. Even though a large volume of ethanol is used to synthesize the droplets, excess ethanol is easily removed by dialysis or by centrifuging the droplets, decanting the solvent, and resuspension in fresh media. Because the ouzo method can consistently produce phase-change contrast agents with a diameter under 200 nm, we believe the new synthesis method will be attractive for applications in extravascular imaging and ultrasound-based therapies.

Droplet Synthesis:

Droplet formulation is an adaptation of microbubble formulations found in commercially available microbubble contrast agents.[1,12,42,50] Ouzo droplets were synthesized using both liquid and gaseous PFCs. The PFCs used included perfluorohexane (C_6F_{14}, $T_{Boiling}$ = 56°C, PFH), perfluoropentane (C_5F_{12}, $T_{Boiling}$ = 29°C, PFP), perfluorobutane (C_4F_{10}, $T_{Boiling}$ = −2°C, PFB), and perfluoropropane (C_3F_8, $T_{Boiling}$ = −37°C, OFP). All PFCs were purchased from SynQuest Laboratories. An initial lipid dissolved in ethanol stock solution was prepared using a 20:1 molar ratio of dipalmitoylphosphatidylcholine (DPPC, CAS: 63-89-8, NOF America Corp.) and N-(Methylpolyoxyethylene oxycarbonyl)-1,2-distearoyl-sn-glycero-3-phosphoethanolamine sodium salt (DSPE-PEG 2K, NOF America Corp.). The lipid concentration varied from 0.10 mg/ml up to 1.82 mg/ml depending on the volume of perfluorocarbon used in the synthesis.

The lipid-ethanol stock solution was then divided as needed. Using a stir plate, PFCs were then dissolved in the lipid-ethanol solution until it was fully saturated. For liquid PFCs (i.e. PFH and PFP), the PFC oil was incrementally added to the stirred ethanol solution until a small droplet of PFC formed in solution. The solution was then removed from the stir plate and allowed to rest at room temperature for approximately 20 minutes, enabling excess PFC to fall to the bottom of the container. For gaseous PFCs (i.e. PFB and OFP), PFC gas was bubbled into a sealed glass vial with the ethanol solution at a pressure of 1.5-2.0 PSI while on ice. It was bubbled through for a minimum of 2 minutes and purged 3 times to ensure the headspace was filled with gaseous PFC. Then, the PFC-lipid-ethanol solution was pipetted into a clean glass vial and diluted as needed using additional lipid-ethanol solution to achieve the desired PFC in ethanol saturation percentage. Finally, a 7:2:1 volume ratio blend of water, propylene glycol (CAS: 57-55-6, Sigma Aldrich), and glycerol (CAS: 56-81-5, Bio-Rad) was added to the solution to nucleate PFC droplets. Prior to measurements, the droplet samples were centrifuged, decanted, and resuspended to separate the droplets from excess alcohol and lipids. This process was repeated 3 times.

Droplet Size and Zeta Potential Measurements:

Droplet size distributions were measured using dynamic light scattering (DLS, Zetasizer NanoZS, Malvern Instruments Ltd., Worcestershire, UK) at 20°C. All samples were allowed to equilibrate in the sample holder for one to five minutes prior to measurement. Viscosity differences in solvent mixtures were corrected for by directly measuring the solvent mixture viscosity using a rheometer (Physica MCR301, Anton Paar, Graz, Austria) in a double gap cylinder (Couette) configuration. Droplet concentrations were estimated based on the volume of PFC introduced into the sample divided by the average diameter of the droplets nucleated.

Zeta potential measurements (Zetasizer NanoZS, Malvern Instruments Ltd., Worcestershire, UK) were all taken at 20°C. Droplet samples with a lipid shell were centrifuged and resuspended three times to remove any possible excess lipids in solution.

Acoustic Activation Threshold Measurements:

A passive cavitation detection method was used to detect droplet activation thresholds. [31,34] Samples were held in a custom built thin-walled plastic cuvette (1 cm diameter, 4 cm long) submerged in a degassed water tank heated to body temperature (37°C). Each sample was diluted to a concentration of approximately 10^8 droplet/ml using degassed 0.45 μm filtered deionized water. To prevent droplet depletion due to vaporization, the sample holder was periodically flushed with deionized water and refilled with a new sample from the same batch. Depending on the acoustic pressure, samples were exchanged after a minimum of 200 and maximum of 1000 acoustic firings.

Droplets were activated using a 1.24 MHz spherically focused ultrasound transducer (H-102, f-number = 0.95, D = 68 mm, Sonic-Concepts Inc., Woodinville, WA, USA). It was driven using a 15-cycle sine wave pulse generated from an arbitrary function generator (AFG 3022, Tektronix, Beaverton, OR, USA) and amplified by 55 dB using an RF amplifier (A-150,

ENI, E&I Ltd., Rochester, NY, USA). Ultrasound pulses were delivered to samples with peak negative pressures ranging from 0 to 7.2 MPa at a pulse repetition frequency of 20 Hz.

Cavitation (activation) signals were detected using a custom-built, unfocused polyvinylidene difluoride (PVDF) transducer with near constant bandwidth up to 40 MHz. The PVDF transducer was positioned 35 mm away from the center of the sample holder orthogonal to the transmitting ultrasound transducer. Signals from this transducer were digitized and collected using a Gage card (Razor 14, Dynamic Systems LLC, Lockport, IL, USA).

Cavitation analysis leveraged the methods of Arnal *et al.* and Li *et al.*[31,34] A 15 μs window, offset by the expected time delay for a one-way time of flight from the focused transducer to the sample then to the PVDF transducer, was used to analyze received ultrasound signals. The cavitation signal was identified by subtracting an averaged background acoustic signal from the signal acquired. A minimum of 200 acoustic signals were used for each acoustic condition for each sample. A cavitation event was identified as an average acoustic intensity 9 times greater than the background noise level. The cavitation (activation) probability was defined as the percentage of cavitation events registered versus the total number of acoustic pulses fired for a given acoustic condition. The activation threshold was defined as the 50% crossing found on a sigmoid fit of the cavitation probability versus pressure data collected.

In Vivo Imaging:

Surgical procedures were performed according to approved institutional animal care and use committee (IACUC) protocol following all appropriate guidelines from the university's Animal Welfare Assurance (A3464–01) as well as the NIH Office of Laboratory Animal Welfare (OLAW). A 0.2 ml bolus injection of perfluorobutane droplets diluted to approximately 10^6 droplet/ml was injected via tail vein in an anesthetized female Sprague-Dawley rat. An ultrasound imaging window was made by performing a laminectomy to expose the spinal cord between T6 and T10. Activated droplets were imaged using a Verasonics Vantage ultrasound system (Verasonics Inc, Bothell, WA, USA) and a 15 MHz transducer (Vermon, Tours, France). The spinal cord was imaged with conventional B-mode imaging and a plane-wave harmonic sequence used to differentiate the activated droplets from the surrounding tissue.[45,46]

Supplementary Material

Refer to Web version on PubMed Central for supplementary material.

Acknowledgements:

The research performed was primarily supported by the National Institutes of Health under grant R01HL125339. Additional support was provided by National Institutes of Health grants R01EB016034, R01CA170734, R01EB009682, R01HL093140, R01DC010201, and R01EY026532 as well as the Life Sciences Discovery Fund 3292512, Royalty Research Fund Grant (RRF-65-3210) and the Washington State Spinal Cord Injury Consortium (WASCIC).

References:

(1). Ferrara K; Pollard R; Borden M Annu. Rev. Biomed. Eng 2007, 9 (1), 415–447. [PubMed: 17651012]

(2). Unger EC; Porter T; Culp W; Labell R; Matsunaga T; Zutshi R Adv. Drug Deliv. Rev 2004, 56 (9), 1291–1314. [PubMed: 15109770]

(3). Wei K; Jayaweera AR; Firoozan S; Linka A; Skyba DM; Kaul S Circulation 1998, 97 (5), 473–483. [PubMed: 9490243]

(4). Cavalli R; Bisazza A; Trotta M; Argenziano M; Civra A; Donalisio M; Lembo D Int. J. Nanomedicine 2012, 7, 3309–3318. [PubMed: 22802689]

(5). Lepeltier E; Bourgaux C; Couvreur P Adv. Drug Deliv. Rev 2014, 71, 86–97. [PubMed: 24384372]

(6). Gao Y; Hernandez C; Yuan H-X; Lilly J; Kota P; Zhou H; Wu H; Exner AA Nanomedicine 2017, 13 (7), 2159–2168. [PubMed: 28603079]

(7). Perera RH; Wu H; Peiris P; Hernandez C; Burke A; Zhang H; Exner AA Nanomedicine 2017, 13 (1), 59–67. [PubMed: 27565686]

(8). Wu H; Rognin NG; Krupka TM; Solorio L; Yoshiara H; Guenette G; Sanders C; Kamiyama N; Exner AA Ultrasound Med. Biol 2013, 39 (11), 2137–2146. [PubMed: 23932272]

(9). Rapoport N; Nam K-H; Gupta R; Gao Z; Mohan P; Payne A; Todd N; Liu X; Kim T; Shea J; Scaife C; Parker DL; Jeong E-K; Kennedy AM J. Control. Release 2011, 153 (1), 4–15. [PubMed: 21277919]

(10). Kripfgans OD; Fowlkes JB; Miller DL; Eldevik OP; Carson PL Ultrasound Med. Biol 2000, 26 (7), 1177–1189. [PubMed: 11053753]

(11). de Gracia Lux C; Vezeridis AM; Lux J; Armstrong AM; Sirsi SR; Hoyt K; Mattrey RF RSC Adv. 2017, 7 (77), 48561–48568. [PubMed: 29430294]

(12). Mountford PA; Borden MA Adv. Colloid Interface Sci 2016, 237, 15–27. [PubMed: 27574721]

(13). Kripfgans OD; Fabiilli ML; Carson PL; Fowlkes JB J. Acoust. Soc. Am 2004, 116 (1), 272–281. [PubMed: 15295987]

(14). Wong ZZ; Kripfgans OD; Qamar A; Fowlkes JB; Bull JL Soft Matter 2011, 7 (8), 4009.

(15). Li DS; Kripfgans OD; Fabiilli ML; Brian Fowlkes J; Bull JL Appl. Phys. Lett 2014, 104 (6), 063703. [PubMed: 24711671]

(16). Qamar A; Wong ZZ; Fowlkes JB; Bull JL Appl. Phys. Lett 2010, 96 (14), 143702. [PubMed: 20448802]

(17). Miles CJ; Doering CR; Kripfgans OD J. Appl. Phys 2016, 120 (3), 034903.

(18). Wei C; Xia J; Lombardo M; Perez C; Arnal B; Larson-Smith K; Pelivanov I; Matula T; Pozzo L; O'Donnell M Opt. Lett 2014, 39 (9), 2599. [PubMed: 24784055]

(19). Matsunaga TO; Sheeran PS; Luois S; Streeter JE; Mullin LB; Banerjee B; Dayton PA Theranostics 2012, 2 (12), 1185–1198. [PubMed: 23382775]

(20). Sheeran PS; Wong VP; Luois S; McFarland RJ; Ross WD; Feingold S; Matsunaga TO; Dayton PA Ultrasound Med. Biol 2011, 37 (9), 1518–1530. [PubMed: 21775049]

(21). Sheeran PS; Luois SH; Mullin LB; Matsunaga TO; Dayton PA Biomaterials 2012, 33 (11), 3262–3269. [PubMed: 22289265]

(22). Samuel S; Duprey A; Fabiilli ML; Bull JL; Fowlkes JB Microcirculation 2012, 19 (6), 501–509. [PubMed: 22404846]

(23). Seda R; Li DS; Fowlkes JB; Bull JL Ultrasound Med. Biol 2015, 41 (12), 3241–3252. [PubMed: 26403698]

(24). Zhang M; Fabiilli ML; Haworth KJ; Fowlkes JB; Kripfgans OD; Roberts WW; Ives KA; Carson PL Ultrasound Med. Biol 2010, 36 (10), 1691–1703. [PubMed: 20800939]

(25). Vlaisavljevich E; Durmaz YY; Maxwell A; Elsayed M; Xu Z Theranostics 2013, 3 (11), 851–864. [PubMed: 24312155]

(26). Zhang P; Porter T Ultrasound Med. Biol 2010, 36 (11), 1856–1866. [PubMed: 20888685]

(27). Fabiilli ML; Lee JA; Kripfgans OD; Carson PL; Fowlkes JB Pharm. Res 2010, 27 (12), 2753–2765. [PubMed: 20872050]

(28). Yu J; Chen X; Villanueva FS; Kim K Appl. Phys. Lett 2016, 109 (24), 243701.

(29). Chen Y-S; Yoon SJ; Frey W; Dockery M; Emelianov S Nat. Commun 2017, 8, 15782. [PubMed: 28593942]

(30). Wilson K; Homan K; Emelianov S Nat. Commun 2012, 3, 618. [PubMed: 22233628]

(31). Li DS; Yoon SJ; Pelivanov I; Frenz M; O'Donnell M; Pozzo LD; O'Donnell M; Pozzo LD Nano Lett. 2017, 17 (10), 6184–6194. [PubMed: 28926276]

(32). Luke GP; Hannah AS; Emelianov SY Nano Lett. 2016, 16 (4), 2556–2559. [PubMed: 27035761]

(33). Fabiilli ML; Haworth KJ; Fakhri NH; Kripfgans OD; Carson PL; Fowlkes JB IEEE Trans. Ultrason. Ferroelectr. Freq. Control 2009, 56 (5), 1006–1017. [PubMed: 19473917]

(34). Arnal B; Perez C; Wei C-W; Xia J; Lombardo M; Pelivanov I; Matula TJ; Pozzo LD; O'Donnell M Photoacoustics 2015, 3 (1), 3–10. [PubMed: 25893169]

(35). Arnal B; Wei C-W; Perez C; Nguyen T-M; Lombardo M; Pelivanov I; Pozzo LD; O'Donnell M Photoacoustics 2015, 3 (1), 11–19. [PubMed: 25893170]

(36). Phillips R; Harris G Information for Manufacturers Seeking Marketing Clearance of Diagnostic Ultrasound Systems and Transducers; Rockville, MD, 2008.

(37). Shpak O; Verweij M; Vos HJ; de Jong N; Lohse D; Versluis M Proc. Natl. Acad. Sci. U. S. A 2014, 111 (5), 1697–1702. [PubMed: 24449879]

(38). Dove JD; Mountford PA; Murray TW; Borden MA Biomed. Opt. Express 2014, 5 (12), 4417. [PubMed: 25574448]

(39). Vitale SA; Katz JL Langmuir 2003, 19 (10), 4105–4110.

(40). François G; Katz JL Chemphyschem 2005, 6 (2), 209–216. [PubMed: 15751338]

(41). Daeichin V; van Rooij T; Skachkov I; Ergin B; Specht PAC; Lima A; Ince C; Bosch JG; van der Steen AFW; de Jong N; Kooiman K IEEE Trans. Ultrason. Ferroelectr. Freq. Control 2017, 64 (3), 555–567. [PubMed: 28113312]

(42). De Cock I; Zagato E; Braeckmans K; Luan Y; de Jong N; De Smedt SC; Lentacker IJ Control. Release 2015, 197, 20–28.

(43). Israelachvili JN Intermolecular and Surface Forces, 3rd ed.; Academic Press: Waltham, MA, 2011.

(44). Lee Y-T; Li DS; Ilavsky J; Kuzmenko I; Jeng G-S; O'Donnell M; Pozzo LD J. Colloid Interface Sci 2019, 536, 281–290. [PubMed: 30380428]

(45). Tremblay-Darveau C; Williams R; Milot L; Bruce M; Burns PN IEEE Trans. Ultrason. Ferroelectr. Freq. Control 2014, 61 (12), 1988–2000. [PubMed: 25474775]

(46). Khaing ZZ; Cates LN; DeWees DM; Hannah A; Mourad P; Bruce M; Hofstetter CP J. Neurosurg. Spine 2018, 1–8.

(47). Hannah AS; VanderLaan D; Chen Y-S; Emelianov SY Biomed. Opt. Express 2014, 5 (9), 3042. [PubMed: 25401018]

(48). Strohm E; Rui M; Gorelikov I; Matsuura N; Kolios M Biomed. Opt. Express 2011, 2 (6), 1432. [PubMed: 21698007]

(49). Wei C; Lombardo M; Larson-Smith K; Pelivanov I; Perez C; Xia J; Matula T; Pozzo D; O'Donnell M Appl. Phys. Lett 2014, 104 (3), 033701. [PubMed: 24753620]

(50). Borden MA; Kruse DE; Caskey CF; Zhao S; Dayton PA; Ferrara KW IEEE Trans. Ultrason. Ferroelectr. Freq. Control 2005, 52 (11), 1992–2002. [PubMed: 16422411]

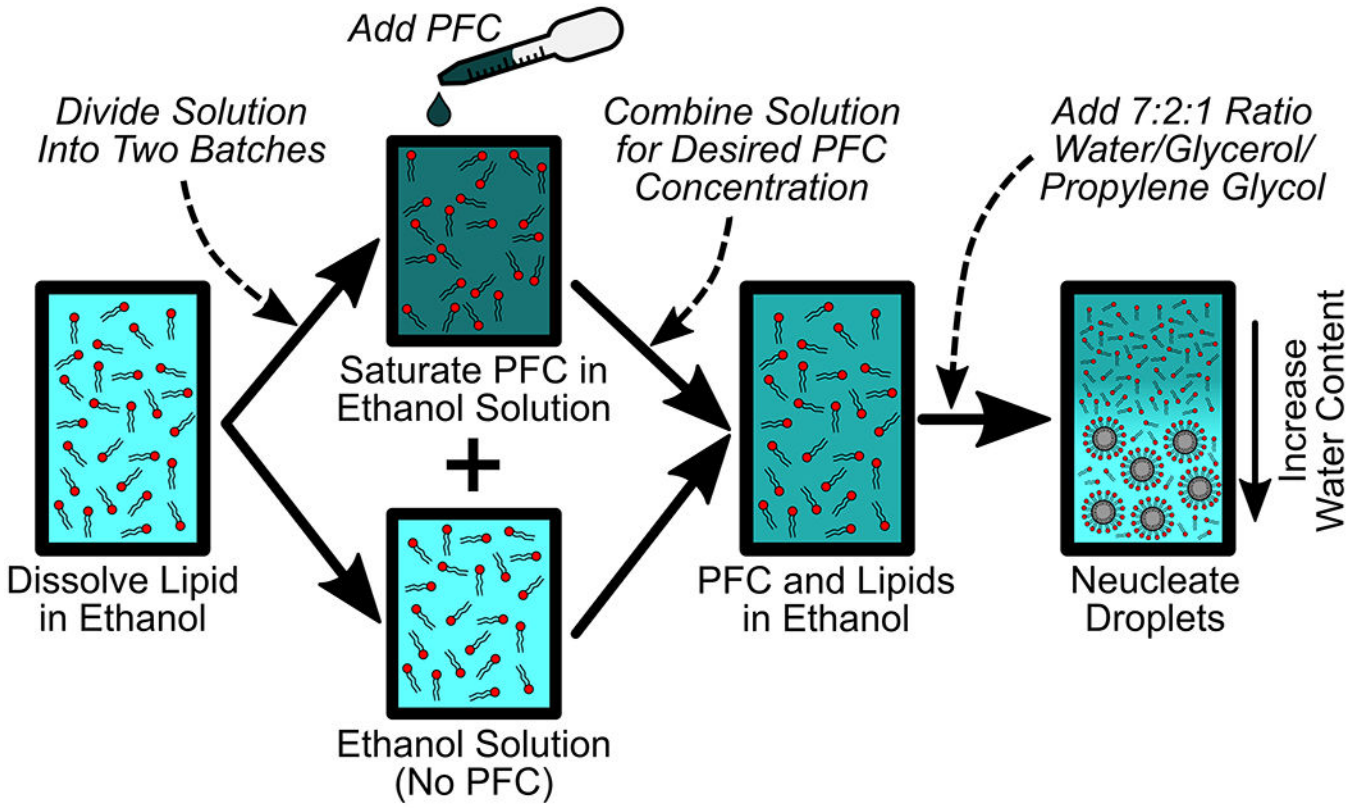

Figure 1:

The ouzo method for PFC nanodroplet production is a process for the spontaneous nucleation of liquid nanodroplets in solution. A lipid surfactant, or any other stabilizer, is first dissolved in ethanol. This solution is then divided such that only one solution is fully saturated with perfluorocarbon. The fully saturated PFC solution and the pure lipid in ethanol solution are re-combined to achieve a desired PFC concentration in the solution. Finally, a water-based solution is pipetted into the container with PFC and lipid dissolved in ethanol. Introducing water causes the PFC to lose solubility, leading to PFC nanodroplet nucleation. This process can be performed with any perfluorocarbon gas or liquid in combination with any surfactant or shell coating.

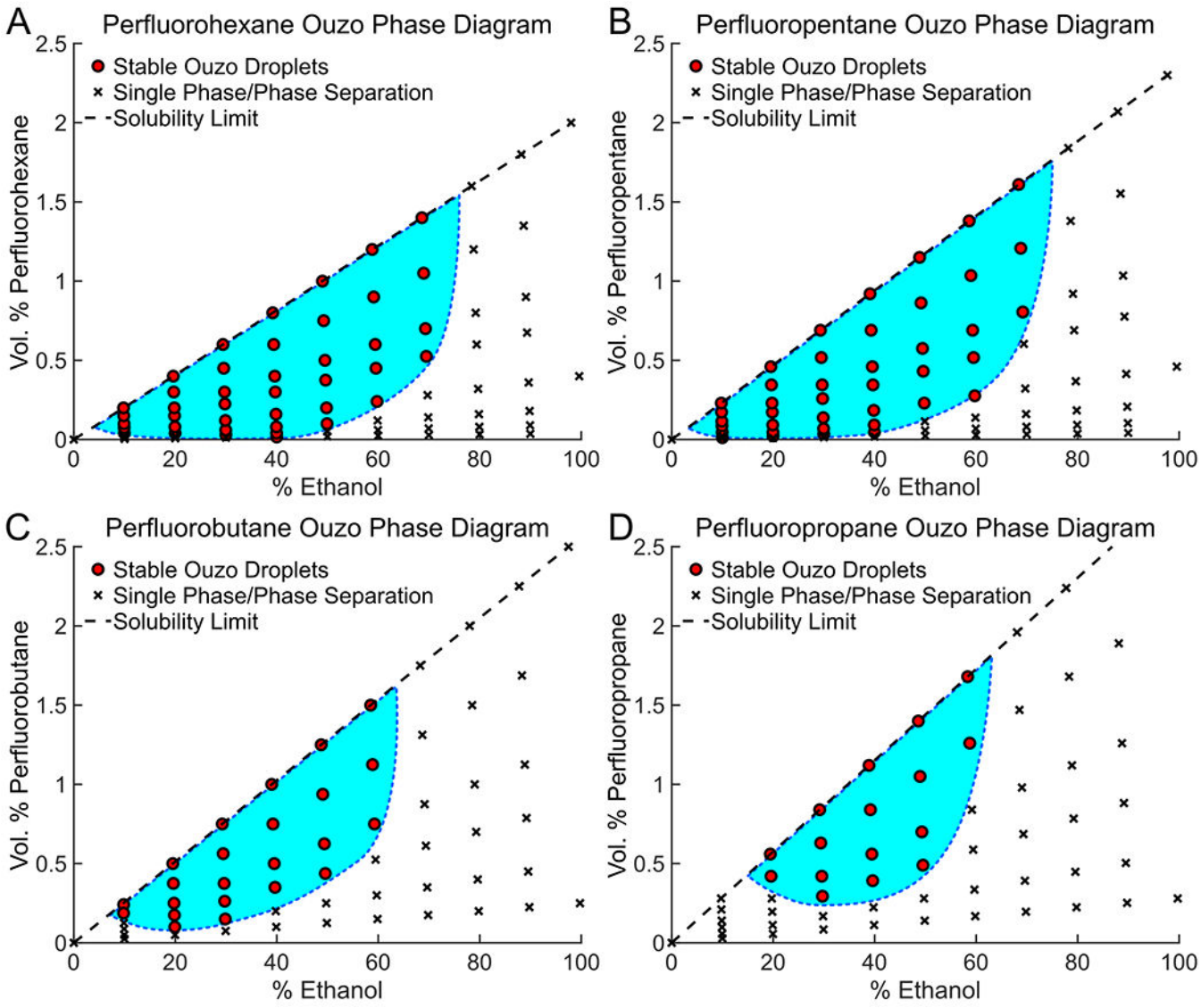

Figure 2:

Ouzo phase diagrams for (A) perfluorohexane, (B) perfluoropentane, (C) perfluorobutane, and (D) perfluoropropane. The ouzo region (conditions leading to droplet formation) is identified with the light blue filled area with a dotted line boarder. Droplets nucleate in a narrow region relative to the entire ternary diagram (see supplemental figure 1).

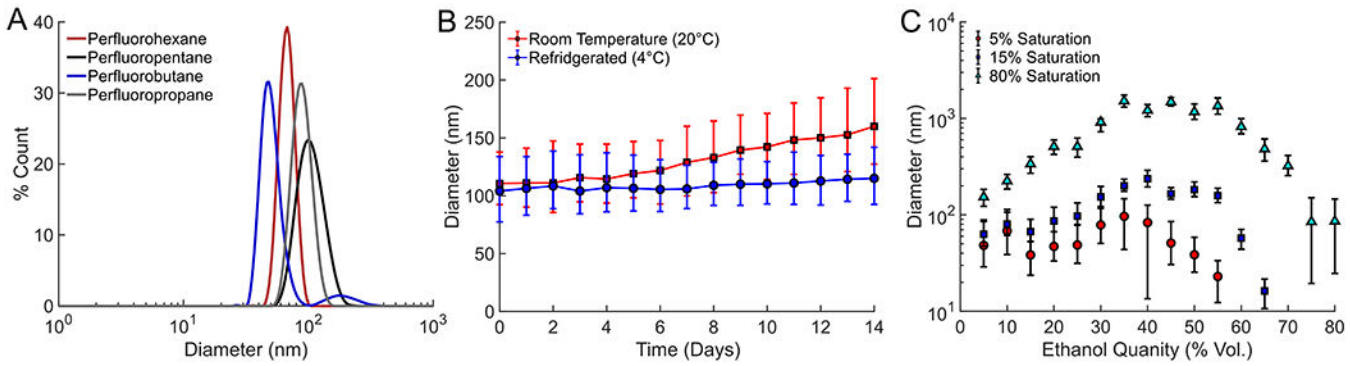

Figure 3:

(A) Size distribution measured using dynamic light scattering of various PFCs prepared using the ouzo synthesis method, (B) size evolution of droplets stored at room temperature or refrigerated over time, and (C) average size of perfluorohexane droplets synthesized as a function of ethanol and PFC saturation in ethanol prior to nucleation. The error bars represent one standard deviation of the size distribution.

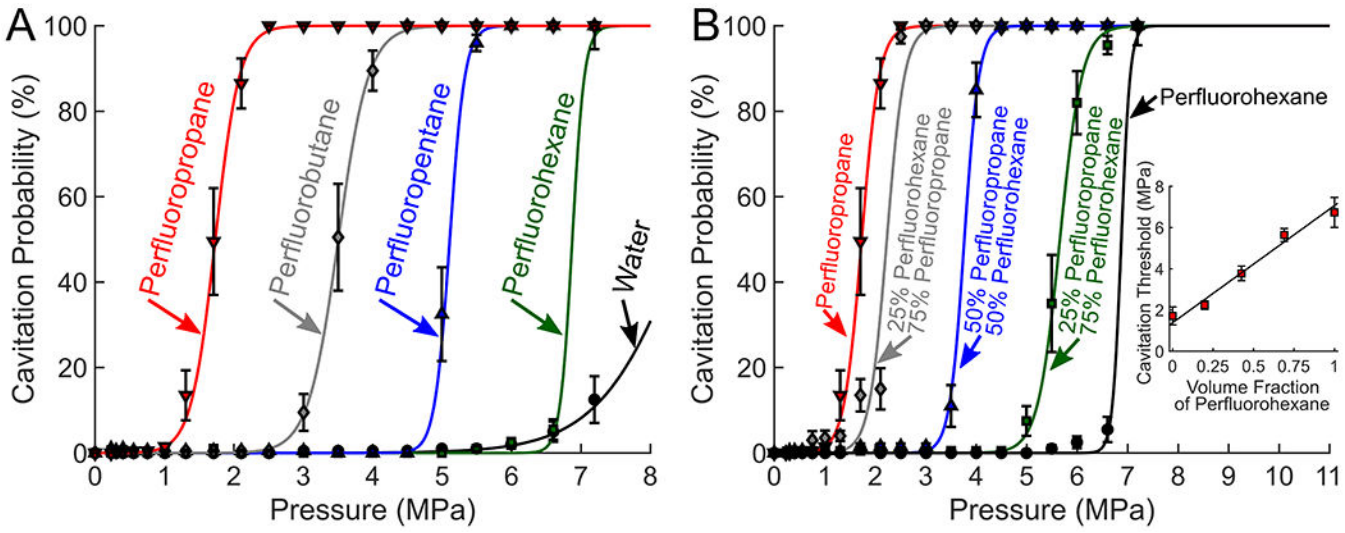

Figure 4:

(A) Cavitation thresholds of pure PFC droplets compared to water and (B) cavitation thresholds using perfluorocarbon mixtures. The inset figure in panel B shows the 50% cavitation threshold of the droplets as a function of perfluorohexane and perfluorobutane mixture ratios. The cavitation threshold of the PFC blended droplets fit the linear function of $P_{Threshold} = P_{PFC_1} V_f + P_{PFC_2}(1 - V_f)$, where P_{PFC_1} and P_{PFC_2} are the activation threshold for the two perfluorocarbons used (in this case perfluorohexane and perfluorobutane), and V_f represents the volume fraction of perfluorohexane. Using the linear fit an R-squared of 0.975 was obtained, suggesting that the activation threshold for the PFC blend could be predicted with a volume mixing ratio.

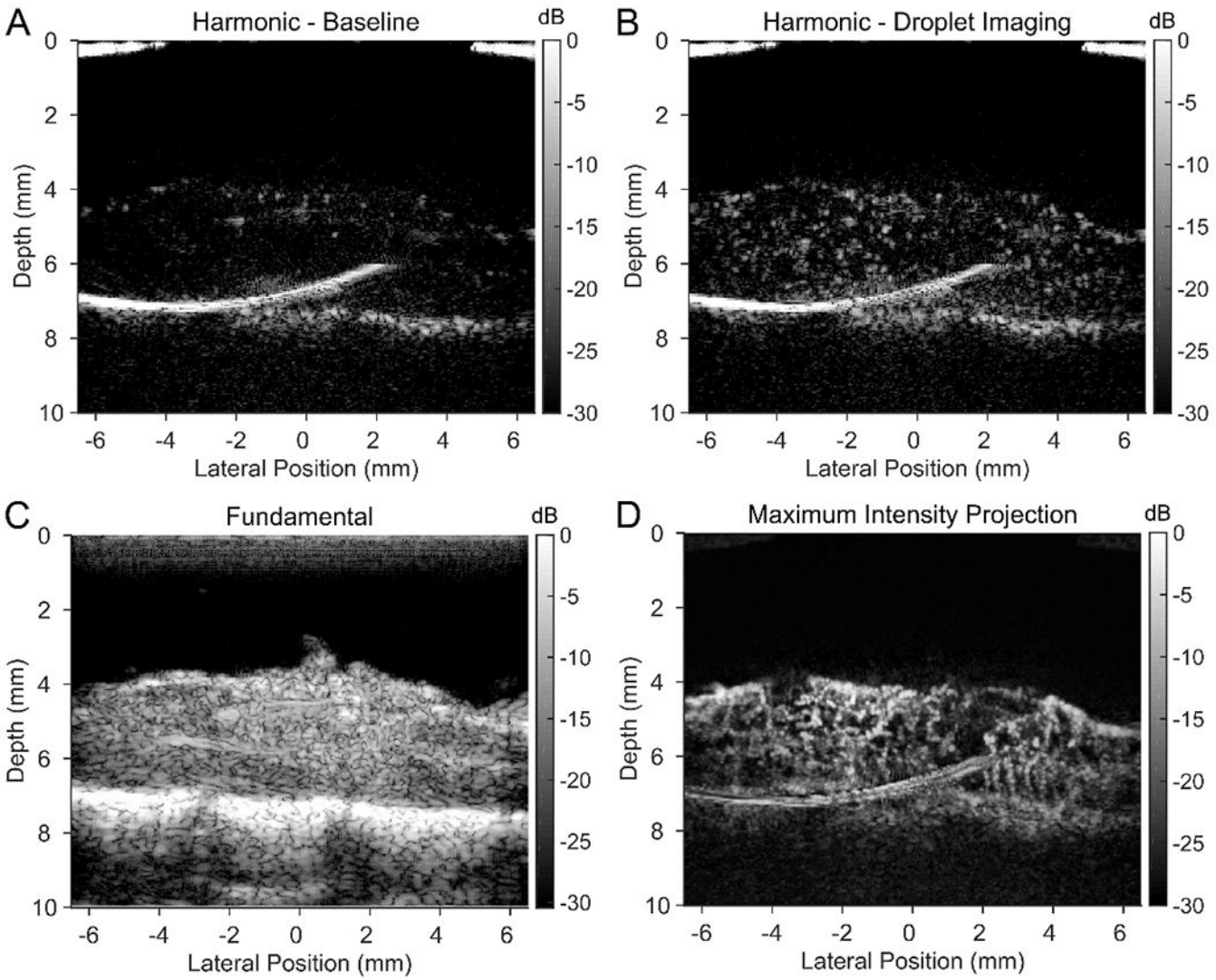

Figure 5:

The spinal cord of a rat model was imaged using a 15 MHz linear array. A bolus injection of perfluorobutane droplets active in the region of interest was highlighted using plane-wave harmonic imaging (A and B) in conjunction with conventional ultrasound imaging (C). (A) Prior to injection, harmonic imaging reveals no contrast, confirming the absence of bubbles. (B) Seconds after injection, individual activated droplets are seen passing through the spinal cord vasculature. (D) After performing a maximum intensity projection of perfusing activated droplets (i.e., bubbles), microvessels were traced out over the image region. See supplemental media for video of activated droplets perfusing the spinal cord using harmonic imaging.